


# **Ligand Sequential Replacement on Chromium(III)-Aqua Complexes by L-Alanine and Other Biological Amino Acids: A Kinetic Perspective**

Joaquin F. Perez-Benito\* and Guillem Martinez-Cereza

Departamento de Ciencia de Materiales y Quimica Fisica, Seccion de Quimica Fisica,  
Facultad de Quimica, Universidad de Barcelona, Marti i Franques, 1, 08028 Barcelona,  
Spain

 *Supporting Information*

---

**ABSTRACT:** The ligand sequential replacement on chromium(III)-aqua complexes by L-alanine in slightly acidic aqueous solutions (pH range: 3.55–5.61) has been kinetically followed by means of UV-Vis spectrophotometry. A two rate constant model has been applied to fit the absorbance-time data, corresponding to the formation ( $k_1$ ) and decay ( $k_2$ ) of an intermediate not reactive enough to be in steady state (long-lived intermediate). The kinetic orders of the amino acid were fractional ( $0.40 \pm 0.03$  for  $k_1$  and  $0.40 \pm 0.02$  for  $k_2$ ). The two steps showed base catalysis, and the activation energies were  $60 \pm 3$  (for  $k_1$ ) and  $83 \pm 6$  (for  $k_2$ )  $\text{kJ mol}^{-1}$ . The rate constants for the coordination of the first L-alanine ligand followed the sequence  $\text{CrOH}^{2+} < \text{Cr(OH)}_2^+ < \text{Cr(OH)}_3$ ,  $\text{Cr}^{3+}$  being almost inactive. This suggests that the increase in the reaction rate with increasing pH was caused by the enhancement of the lability of the Cr(III)-aqua bonds induced by the presence of hydroxo ligands. The activation parameters for a series of ligand substitution on Cr(III)-aqua complexes by organic molecules yielded a statistically significant enthalpy-entropy linear plot with an isokinetic temperature of  $296 \pm 21$  K.

---

## 1. INTRODUCTION

The coordination chemistry of chromium(III) differs from those of other transition metal ions in the rate of the reaction between the metal and its ligands. Whereas chemists are used to see in their laboratories how typical complexes such as tetraamminecopper(II) or diamminesilver(I) ions form in a rather fast way, and kinetic studies of the substitution of coordinated water on Pt(II) and many other metal ions by organic ligands often require the use of rapid reactant mixing techniques as the stopped-flow method,<sup>1</sup> the characteristic kinetic inertness to substitution of the Cr(III)  $d^2sp^3$  octahedral complexes<sup>2,3</sup> makes them especially attractive candidates to be employed in kinetic studies affordable by ordinary UV-Vis spectroscopy. For instance, the relatively slow reaction between Cr(III) and ethylenediaminetetraacetic acid (EDTA)<sup>4,5</sup> is selected as an adequate experiment in chemical kinetics for undergraduate students in some university faculties around the world.<sup>6,7</sup>

The complexes of Cr(III) are of certain importance in biology. Actually, chromium is nowadays considered by many authors as a necessary nutritional oligoelement<sup>8</sup> because of its participation in the glucose tolerance factor.<sup>9-12</sup> Although the classification as an essential trace element remains polemical,<sup>13,14</sup> the capacity of chromium to potentiate the action of insulin is well established.<sup>15</sup>

On the other hand, L-alanine, the simplest  $\alpha$ -amino acid presenting optical isomerism, is classified as one of the 10 non-essential biological amino acids for humans, due to their ability to produce it.<sup>16</sup> Given that the amino acid molecules exhibit two functional groups with nitrogen and oxygen atoms capable of acting as electron-pair donors, they can be considered as suitable ligands for vacant-orbital transition metal ions. In particular, the reactions of complexation of Cr(III) by amino acids might be related to the problem of the origin of the

first peptides on prebiotic Earth,<sup>17</sup> since transition metal ions have been shown to catalyze the formation of peptide bonds between the amino acid monomers acting as ligands.<sup>18</sup>

The substitution reactions on aqua,<sup>19-26</sup> hydroxo,<sup>27</sup> and ammonia<sup>28</sup> complexes of Cr(III) by amino acids have been the subject of several kinetic studies. Although the results of two independent investigations of the Cr(III)-alanine reaction have already been reported,<sup>29,30</sup> the process under a large excess of organic ligand being classified in both cases as a pseudo-first order reaction, some clear-cut deviations from this simple kinetic behavior have been observed. The main objective of the present work will be to search for and eventually find a kinetic model capable of accounting for those deviations.

## 2. EXPERIMENTAL PART

**2.1. Materials and Methods.** All the experiments were done using milli-Q quality (Millipore Synergy UV system) water as solvent. The source of metal ions required to carry out the kinetic runs was Cr(NO<sub>3</sub>)<sub>3</sub>·9H<sub>2</sub>O (Merck). The source of organic ligands used in most experiments was CH<sub>3</sub>-CH(NH<sub>2</sub>)-COOH (alanine, in its L and DL forms, Sigma-Aldrich). Other amino acids used were glycine (Merck), as well as L-phenylalanine (Sigma-Aldrich), L-threonine (Sigma-Aldrich), and L-histidine (Fluka). KOH (Merck) and HCl (Sigma-Aldrich) were employed to perform the reactions at an adequate pH range. Actually, the window of accessible pHs was rather narrow, being limited at the bottom by the rate of reaction (too slow under very acidic conditions) and at the top by the eventual precipitation of Cr(OH)<sub>3</sub>. The background electrolyte used to change the ionic strength when necessary was KNO<sub>3</sub> (Merck).

The pH measurements were done by means of a Wave pH-meter provided with a combination electrode (calibrated with buffers at pHs 4.00 and 7.00, Sigma-Aldrich). The kinetic runs were monitored by a periodical measurement of the reacting mixture absorbance either at five different wavelengths with a Shimadzu 160 A UV-Vis spectrophotometer or at a single wavelength with a Shimadzu UV-1201V spectrophotometer. At the end of the reactions, the UV-Vis spectra corresponding to the final reaction products were recorded with the aid of a third spectrophotometer (SI Analytics, UV Line 8100 model).

**2.2. Kinetic Experiments and Calculations.** In most of the runs, the complexing agent (either L-alanine or other amino acid) was in large excess with respect to the metal ion, Cr(III), acting as limiting reactant (isolation method). The selected wavelength to follow the reactions (leading to the highest difference between the initial and final absorbance readings) was usually that of 530 nm. The absorbances of the reacting mixture were periodically measured (time intervals: 60-360 s) during at least 6 hours, and the final values, along with the UV-Vis spectrum and the pH, were taken 4 days later (higher delay times were not advisable because of the potential contamination by fungal colonies feeding on the amino acid). All the experimental determinations were duplicated. In total, 106 kinetic runs were performed.

### 3. RESULTS AND DISCUSSION

**3.1. Spectrophotometric Monitoring of the Reaction.** The stock aqueous solution of  $\text{Cr}(\text{NO}_3)_3$  (0.3 M, pH 2.01) exhibited a distinct blue color. Addition of an aliquot to an aqueous mixture of L-alanine and KOH resulted usually in precipitation of  $\text{Cr}(\text{OH})_3$ , which

redissolved rapidly on stirring, yielding a perfectly transparent green solution, whose color shifted gradually to violet as the complexation reaction advanced.

The absorbance of the solution increased at most wavelengths of the UV-Vis spectrum during the course of the reaction, and two absorption peaks shifting gradually toward the left side could be observed (Figure 1). The higher increase of the absorbance was that corresponding to the peak situated at the higher wavelength, thus being the best choice to follow the reaction keeping the experimental errors as low as possible.

In certain kinetic studies, when the reaction has been followed by a spectrophotometric technique determining simultaneously the absorbances at two different wavelengths, a representation of the absorbance at one wavelength,  $A(\lambda_1)$ , as a function of the other,  $A(\lambda_2)$ , can yield some useful information on the chemical system under study, for instance, the participation of a long-lived intermediate (as opposed to very reactive, steady-state intermediates<sup>31-33</sup>) in the mechanism<sup>5</sup> or the colloidal nature of one of the reaction products.<sup>34-</sup>

<sup>36</sup> In the presence of a long-lived intermediate (I), the relationship follows the law:

$$A(\lambda_1) = A(\lambda_1)_o + \frac{\epsilon_{P,1} - \epsilon_{R,1}}{\epsilon_{P,2} - \epsilon_{R,2}} [A(\lambda_2) - A(\lambda_2)_o] + C [I] \quad (1)$$

where:

$$C = \left[ \frac{\epsilon_{I,1} (\epsilon_{P,2} - \epsilon_{R,2}) + \epsilon_{P,1} (\epsilon_{R,2} - \epsilon_{I,2}) + \epsilon_{R,1} (\epsilon_{I,2} - \epsilon_{P,2})}{\epsilon_{P,2} - \epsilon_{R,2}} \right] l \quad (2)$$

$A(\lambda_1)_o$  and  $A(\lambda_2)_o$  being the initial absorbances at the two wavelengths and  $l$  the optical path length, whereas the subscripts of the molar absorption coefficients indicate the corresponding

chemical species (reactant, intermediate, and product) and wavelength. According to eqs 1 and 2, in the absence of any long-lived intermediate ( $[I] = 0$ ) the  $A(\lambda_1)$  vs  $A(\lambda_2)$  plots should be linear. However, in the particular case of the Cr(III)-alanine reaction, both downward-concave ( $\lambda_1 = 585$  nm,  $\lambda_2 = 530$  nm) and upward-concave ( $\lambda_1 = 400$  nm,  $\lambda_2 = 530$  nm) curves (Figure S1) were observed, suggesting the participation of at least a long-lived intermediate in the mechanism.

In all the experiments corresponding to the Cr(III)-alanine reaction (and also for the other amino acids studied, except in the case of L-histidine), the absorbance-time plots presented a downward-concave curvature, meaning that the reaction rate decreased right from the beginning of the process (Figure S2, top). This decrease was much faster than expected for a pseudo-first order reaction (Figure 2). As a consequence, attempted pseudo-first order plots led to nonlinear upward-concave plots (Figure S2, bottom). However, in the case of L-histidine, as well in those previously reported for the reactions of Cr(III) with EDTA<sup>5</sup> and L-glutamic acid,<sup>37</sup> sigmoidal (S-shaped) absorbance vs time and autocatalytic-like (bell-shaped) rate vs time plots were found.

**3.2. Consecutive Steps: A Kinetic Model for the Reaction.** According to the available experimental information, the kinetics of the Cr(III)-alanine reaction seems to follow the simplified mechanism:



where R, I, and P stand for the limiting reactant (the metal ion), the long-lived intermediate (not being reactive enough to be in steady state, the slow step thus being the one corresponding to its decay), and the reaction product, respectively. The exact solutions for the time dependences of the concentrations of these species can be obtained by integration of the corresponding differential equations,<sup>38</sup> and are the following:

$$[\text{R}] = [\text{R}]_0 e^{-k_1 t} \quad (4)$$

$$[\text{I}] = \frac{k_1 [\text{R}]_0}{k_2 - k_1} (e^{-k_1 t} - e^{-k_2 t}) \quad (5)$$

$$[\text{P}] = [\text{R}]_0 - [\text{R}] - [\text{I}] \quad (6)$$

where  $[\text{R}]_0$  is the initial concentration of the limiting reactant. The total absorbance at a given wavelength can be calculated as:

$$A_\lambda = (\varepsilon_{\text{R},\lambda} [\text{R}] + \varepsilon_{\text{I},\lambda} [\text{I}] + \varepsilon_{\text{P},\lambda} [\text{P}]) l \quad (7)$$

where  $\varepsilon_{\text{R},\lambda}$ ,  $\varepsilon_{\text{I},\lambda}$ , and  $\varepsilon_{\text{P},\lambda}$  are the molar absorption coefficients corresponding to the reactant, intermediate, and product, respectively, and considering the initial and final absorbances:



$$A_{\lambda} = \frac{A_{\lambda,0}}{[R]_0} [R] + \varepsilon_{1,\lambda} [I] l + \frac{A_{\lambda,\infty}}{[R]_0} [P] \quad (8)$$

Whereas the value of  $A_{\lambda,\infty}$  could be obtained from the final absorbance reading (once the reacting mixture reached the equilibrium state), that of  $A_{\lambda,0}$  was not experimentally accessible in a direct way because at  $t = 0$  the reactants were still being mixed together. Thus, in a BASIC program different values of four fitting parameters ( $A_{\lambda,0}$ ,  $\varepsilon_{1,\lambda}$ ,  $k_1$  and  $k_2$ ) were systematically changed until minimization of the absorbance average error was attained. The latter was defined as:

$$E = \frac{\sum_{i=1}^N |A_{i,\text{cal}} - A_{i,\text{exp}}|}{N} \quad (9)$$

$A_{i,\text{cal}}$  and  $A_{i,\text{exp}}$  being the calculated and experimental absorbances at different times during the progress of the complexation reaction, respectively, and  $N$  the number of experimental points available for each kinetic experiment. The program so developed yielded a good enough concordance between the calculated and experimental absorbances ( $E = 3.40 \times 10^{-4} - 1.50 \times 10^{-3}$ ).

Furthermore, given that the Cr(III)-alanine reaction (under conditions of a large excess of organic ligand) has been previously reported in the chemical literature to follow a pseudo-first order behavior,<sup>29,30</sup> it might be worth to compare the quality of the absorbance-time fits attained with two mathematical alternatives: the biparametric pseudo-first order kinetic model

(involving  $A_{\lambda,0}$  and  $k$ ) and the tetraparametric model (involving  $A_{\lambda,0}$ ,  $\varepsilon_{1,\lambda}$ ,  $k_1$  and  $k_2$ ) used in the present work. As can be seen in Figure 3, the ratio between the experimental and calculated absorbances during the course of the reaction was much closer to unity when the two rate constant kinetic model was employed, the difference between the two models being especially notable at the beginning of the reaction.

**3.3. Reaction of Cr(III) with L-Alanine Kinetic Results.** Both rate constants decreased as the metal ion initial concentration increased,  $k_1$  according to an upward-concave curve, whereas  $k_2$  yielded a straight line (Figure S3). These decreases were caused by the corresponding decrease in the reacting mixture initial pH, due primarily to the dissociation of hexaaquachromium(III) ion to yield hydroxopentaaquachromium(III) ion.<sup>39,40</sup>

In contrast, both rate constants increased as the organic ligand initial concentration increased. The corresponding double-logarithm plots yielded straight lines with slopes  $0.40 \pm 0.03$  in the case of  $k_1$  and  $0.40 \pm 0.02$  in that of  $k_2$  (Figure 4). This means that the apparent kinetic orders of the amino acid were fractional (non-integer) numbers, thus excluding the possibility of the reaction being of first order as far as the concentration of L-alanine was concerned.

The ionic strength of the medium was changed by the use of  $\text{KNO}_3$  as background electrolyte, and its effects on both experimental rate constants have been determined. A plot of the logarithm of each magnitude against  $I^{1/2}/(1+I^{1/2})$  yielded straight lines with the slopes  $0.93 \pm 0.18$  (for  $k_1$ ) and  $-0.43 \pm 0.26$  (for  $k_2$ )  $\text{M}^{-1/2}$  (Figure S4).

The pH of the medium was varied by means of a changing concentration of KOH. An increase of the pH resulted in an increase of both  $k_1$  and  $k_2$  (Figure 5), indicating the existence of base catalysis in the two cases.

Both experimental rate constants increased with increasing temperature (Table 1), fulfilling the Arrhenius equation (Figure S5), and yielding an activation energy for the first experimental rate constant considerably lower than that associated with the second (Table 2). This result is consistent with the finding that rate constant  $k_1$  was one order of magnitude higher than  $k_2$ .

On the other hand, when the source of organic ligands was changed from L-alanine to a DL-alanine racemic mixture, both the kinetic data ( $k_1$  and  $k_2$ ) and the final UV-Vis spectrum remained unaltered within the experimental error margin (Figure S6), denoting that the reaction was rather insensitive to the nature of the amino acid optical isomer.

**3.4. Reactions of Cr(III) with Other Amino Acids: Kinetic Results.** The temperature-dependence kinetic data for the reactions of Cr(III) with four other biological amino acids have been determined, fulfilling in all the cases the Arrhenius equation (Figure S5) and yielding the activation parameters compiled in Table 2. Whereas the reactions with glycine, L-phenylalanine, and threonine followed the same two rate constant kinetic model developed for that with L-alanine (involving a single long-lived intermediate), the reaction with L-histidine followed a three rate constant kinetic model (involving two long-lived intermediates). These three rate constants were designated as  $k_0$ ,  $k_1$ , and  $k_2$ . Whereas rate constants  $k_1$  and  $k_2$  for L-histidine correlated well with their counterparts for the other four amino acids (Figure 6), rate constant  $k_0$  followed a different pattern. This suggests that the discordant rate constant did not correspond actually to the replacement of an aqua ligand by the amino acid but to the base-catalyzed aquation of an initial Cr(III)-nitrate complex<sup>41,42</sup> (rate constant  $k_0$ ) instead, the Cr(III)-aqua complex being the one susceptible of reaction with a first amino acid molecule (rate constant  $k_1$ ) followed by a second (rate constant  $k_2$ ).

A representation of the activation enthalpy as a function of the activation entropy for the reactions of Cr(III) with EDTA,<sup>5</sup> L-glutamic acid,<sup>37</sup> and the five amino acids corresponding to the present study yielded a linear plot (Figure 7). It has been shown, however, that at least some of the enthalpy-entropy linear correlations found in the chemical literature are caused by the accumulation of experimental errors. This is so because the standard deviation associated with the enthalpy is directly proportional to that associated with the entropy, the proportionality constant being equal to the mean experimental temperature.<sup>43-47</sup> Nevertheless, there seem to be reliable evidences supporting the physicochemical meaning of some of those correlations.<sup>48,49</sup> In the present case, despite the slope of the plot (isokinetic temperature,  $T_{iso} = 296 \pm 21$  K) being almost coincident with the mean experimental temperature ( $T_{exp} = 298$  K), the correlation was statistically significant since, according to the *p*-test,<sup>50</sup> the probability of it being caused by random experimental errors was relatively low ( $P = 0.0106$ ).

**3.5. UV-Vis Spectrum of the Long-Lived Intermediate.** The electronic spectrum of the long-lived intermediate could not be directly recorded, but it could be calculated by discounting the contributions of both the green reactant and violet product from the spectrum recorded at the instant when the intermediate reached its maximum concentration, by means of the formula:

$$\varepsilon_{I,\lambda} = \frac{A_{\lambda} - (\varepsilon_{R,\lambda} [R]_{max} + \varepsilon_{P,\lambda} [P]_{max}) l}{[I]_{max} l} \quad (10)$$

where  $[R]_{max}$ ,  $[I]_{max}$ , and  $[P]_{max}$  are the concentrations of reactant, intermediate, and product at the instant:

$$t_{\max} = \frac{1}{k_1 - k_2} \ln \frac{k_1}{k_2} \quad (11)$$

As shown in Figure 8, the spectrum was intermediary between those corresponding to the reactant and product. This result contrasts with the spectra for the long-lived intermediates observed in the reactions of Cr(III) with EDTA<sup>5</sup> or L-glutamic acid,<sup>37</sup> since in the latter two cases the spectrum was very close to that recorded for the reactant. This suggests that they might be in fact quite different intermediates, the one involved in the Cr(III)-alanine reaction being a complex with a single amino acid ligand (the product containing two or more organic ligands), whereas the ones involved in both the Cr(III)-EDTA and Cr(III)-glutamic acid reactions might be Cr(III)-aqua complexes containing zero organic ligands, their formation corresponding to the aquation reaction of the initial Cr(III)-nitrate complex, as happened also in the case of the first long-lived intermediate formed in the Cr(III)-histidine reaction.

**3.6. UV-Vis Spectra of the Reaction Products.** The final reaction mixture showed a distinct violet color and, once recorded its spectrum, two strong peaks were observed in the visible region, their wavelengths depending on the experimental conditions. An increase of the Cr(III) initial concentration resulted in a shift of the two absorption peaks recorded for the final violet complex toward higher wavelengths and, as could be easily anticipated, the corresponding maximum absorbances increased indeed, but the plots were not linear, showing a downward-concave curvature instead (Figure S7). In fact, even if the wavelength was kept constant (530 nm), there was a deviation from the Lambert-Beer law, since the molar absorption coefficient decreased as the metal ion initial concentration increased (Figure 9).

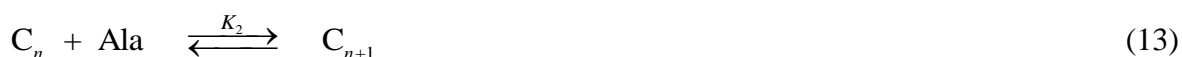
In contrast, an increase of the L-alanine initial concentration resulted in a shift of the two spectral absorption peaks for the final violet complex toward lower wavelengths and, as observed before for the effect of the metal ion initial concentration, the corresponding maximum absorbances increased, but the plots were not linear either, showing a downward-concave curvature again (Figure 10).

The spectral parameters corresponding to the reaction product with Cr(III) coordinated to the highest possible number of organic ligands (saturated) could be obtained by extrapolation of the data shown in Figure S7 at  $[\text{Cr(III)}]_0 = 0$  or of those shown in Figure 10 at  $[\text{L-alanine}]_0 = \infty$ . To check the results, the corresponding extrapolations at either  $[\text{Cr(III)}]_0 = \infty$  or  $[\text{L-alanine}]_0 = 0$ , leading to the spectral parameters corresponding to the reactant with Cr(III) coordinated to zero organic ligands, were also carried out. The extrapolated values so obtained are compiled in Table 3. It should be noticed that the ones obtained at infinite initial concentrations (of either metal ion or amino acid) are to be preferred over those obtained at zero initial concentrations, for they are closer to the experimental values in the case of the reactant (the only species for which the spectrum parameters are directly accessible).

A variation of the initial potassium hydroxide concentration had also an effect on the UV-Vis spectrum of the reaction product mixture. As can be observed, an increase of the initial base concentration resulted in a decrease of the wavelengths associated with the two peaks and an increase of the corresponding absorbances (Figure S8).

The spectroscopic data shown in Figures S7, S8, and 10 indicate that the wavelength for the first visible peak of the final reacting mixture lied in the range 392–409 nm, and for the second in the range 528–548 nm, increasing both with the initial concentration of metal ion and decreasing both with the initial concentrations of either ligand or potassium hydroxide. The values reported for the number of L-alanine ligands coordinated to each Cr(III) center in

the final violet complex are 2 according to some authors<sup>30</sup> and 3 according to others.<sup>29</sup> Actually, the results shown in Figures S7, S8, 9, and 10 cannot be explained unless we assume the presence of at least four different complexes in the final reacting mixture. Thus, although the participation of other complexes cannot be discarded, the simplest explanation for the experimental data so far available is that four complexes differing either in the number of organic ligands or in their acid-base properties coexist in equilibrium in the final reacting mixture:



where  $C_n$  (or  $C_n - H^+$ ) and  $C_{n+1}$  (or  $C_{n+1} - H^+$ ) are Cr(III) complexes involving  $n$  and  $n+1$  L-alanine ligands, respectively, their total concentrations being  $[C_n]_T = [C_n] + [C_n - H^+]$  and  $[C_{n+1}]_T = [C_{n+1}] + [C_{n+1} - H^+]$ . From a mass balance, it follows that:

$$\frac{[C_{n+1} - H^+]}{[C_n - H^+]} = K_1 \{ [Ala]_T - n [C_n]_T - (n+1) [C_{n+1}]_T \} \quad (14)$$

$$\frac{[C_{n+1}]}{[C_n]} = K_2 \{ [Ala]_T - n [C_n]_T - (n+1) [C_{n+1}]_T \} \quad (15)$$

Since an increase of the metal ion initial concentration results in an increase of both  $[C_n]_T$  and  $[C_{n+1}]_T$ , and so in a decrease of the  $[C_{n+1} - H^+]/[C_n - H^+]$  and  $[C_{n+1}]/[C_n]$  ratios, whereas an increase of the L-alanine initial concentration leads to the opposite result (an increase of the

$[C_{n+1}-H^+]/[C_n-H^+]$  and  $[C_{n+1}]/[C_n]$  ratios), eqs 14 and 15 are consistent with the plots shown in Figures S7, 9, and 10 provided that the electronic spectra corresponding to the different complexes are shifted toward lower wavelengths as the number of organic ligands increases and, at the same time, there is an enhancement of the intensity of the absorption peaks:

$$\lambda_{1,2}(0) > \lambda_{1,2}(n) > \lambda_{1,2}(n+1) \quad (16)$$

$$\varepsilon_{1,2}(0) < \varepsilon_{1,2}(n) < \varepsilon_{1,2}(n+1) \quad (17)$$

In eqs 16 and 17 the subscripts correspond to the first and second peaks of the UV-Vis spectrum, and the numbers within parentheses correspond to the L-alanine ligands coordinated to Cr(III) in each of the five complexes proposed: 0 for the initial green complex,  $n$  for the final violet complexes  $C_n-H^+$  or  $C_n$ , and  $n+1$  for the final violet complexes  $C_{n+1}-H^+$  or  $C_{n+1}$ . Moreover, the finding of a clear-cut dependence of the electronic spectrum of the final reacting mixture on the pH of the medium (Figure S8) allows us to infer that:

$$\lambda_{1,2}(C_n) < \lambda_{1,2}(C_n - H^+) \quad (18)$$

$$\lambda_{1,2}(C_{n+1}) < \lambda_{1,2}(C_{n+1} - H^+) \quad (19)$$

$$\varepsilon_{1,2}(C_n) > \varepsilon_{1,2}(C_n - H^+) \quad (20)$$

$$\varepsilon_{1,2}(C_{n+1}) > \varepsilon_{1,2}(C_{n+1} - H^+) \quad (21)$$



**3.7. Hydrogen Ions Released.** The number of hydrogen ions released to the medium per chromium atom during the course of the reaction could be calculated from the value of  $\text{pH}_\infty$  by means of the following equation:

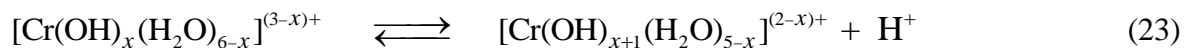
$$\text{Number (H}^+) = \left\{ \left( \frac{[\text{L}]_0 - n [\text{M}]_0}{K_a + [\text{H}^+]_\infty} + 1 \right) [\text{H}^+]_\infty + [\text{B}]_0 \right\} \frac{1}{[\text{M}]_0} \quad (22)$$

where L, B, and M stand for ligand, base (potassium hydroxide) and metal, respectively,  $n$  is the number of organic ligands coordinated per chromium atom, and  $K_a$  is the first acid-dissociation equilibrium constant of protonated L-alanine (for the carboxyl group,  $\text{p}K_a$  2.35 at 25.0 °C).<sup>51,52</sup> The results indicated that the number of hydrogen ions released per chromium atom decreased as the initial concentration of metal ion increased, whereas it increased as the initial concentrations of either L-alanine or potassium hydroxide increased, remaining within the range  $0.73 \leq \text{Number (H}^+) \leq 2.53$  (Figure 11).

**3.8. Chromium(III) Speciation.** The kinetics of the reaction between Cr(III) and L-alanine resembles that of other similar processes, such as the complexations of the same metal ion by EDTA<sup>5</sup> or the  $\alpha$ -amino acids L-glutamic acid,<sup>26,37</sup> DL-leucine,<sup>25</sup> and DL-lysine,<sup>26</sup> in that all of them exhibit base catalysis. It is precisely this pH dependence that offers the main clue to elucidate the mechanism involved in the reaction.

Trivalent chromium finds itself in slightly acidic aqueous solutions in the form of several species in equilibrium, from hexaaquachromium(III) ion to dissolved (either monomolecular

or colloidal) chromium(III) hydroxide, passing through the monohydroxo and dihydroxo complexes:



where  $x = 0-2$ . Although the corresponding equilibrium constants were not known with exactitude for some time,<sup>53</sup> a recent publication has reported experimental values for them that can be considered as reliable (for the successive dissociations of the hexaaqua complex:  $\text{p}K_{\text{a},1}$  3.52,  $\text{p}K_{\text{a},2}$  5.78,  $\text{p}K_{\text{a},3}$  7.88).<sup>54</sup>

Since, according to the kinetic model developed in the present work, rate constant  $k_1$  should be considered as the ratio between the initial values of the reaction rate and the concentration of the inorganic (limiting) reactant, it must be correlated with the initial pH of the reacting mixtures. Unfortunately, given the slow response of the pH meter to yield accurate measurements, the only pH data experimentally accessible with a high degree of confidence are those corresponding to an equilibrium state ( $\text{pH}_\infty$ ). However, the initial pH for each kinetic run could be theoretically calculated from the first and second acid-dissociation equilibrium constants of hexaaquachromium(III) ion<sup>54</sup> and the first of the protonated form of L-alanine.<sup>51,52</sup> It should be noticed that the use of a buffer was not advised because of the potential competition between the anionic basic form of the buffer and L-alanine as ligands for the metal ion.

The relative fractions of the different Cr(III) species present in equilibrium within the initial pH range covered by our kinetic experiments are shown in Figure S9. The predominant form was the monohydroxo complex, with appreciable amounts of both the hexaaqua and

dihydroxo complexes, and the hydroxide in very small concentration. In a first trial, we attempted to calculate the value of experimental rate constant  $k_1$  as a linear combination of the contributions of the four possible Cr(III) species:

$$k_{1,\text{cal}} = \frac{\sum_{x=0}^3 k_{1,x} [\text{Cr}(\text{OH})_x (\text{H}_2\text{O})_{6-x}^{(3-x)+}]}{\sum_{x=0}^3 [\text{Cr}(\text{OH})_x (\text{H}_2\text{O})_{6-x}^{(3-x)+}]} \quad (24)$$

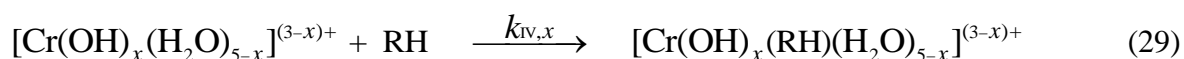
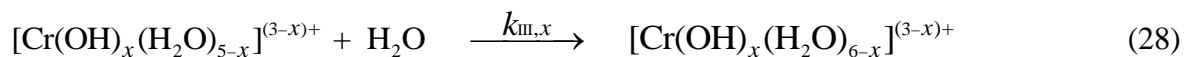
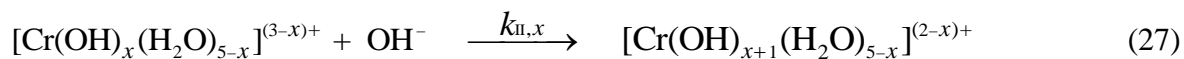
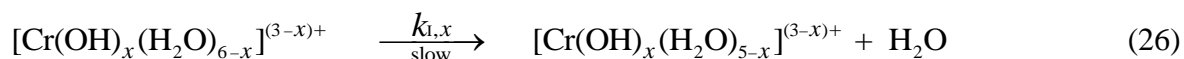
A BASIC program was developed in order to find the best set of values  $k_{1,x}$  ( $x = 0-3$ ) minimizing the difference between the calculated ( $k_{1,\text{cal}}$ ) and experimental ( $k_{1,\text{exp}}$ ) rate constants. However, a  $k_{1,\text{exp}}$  vs.  $k_{1,\text{cal}}$  plot yielded a downward-concave curve (Figure 12, top). Therefore, a second trial was made (considering now negligible the contribution corresponding to  $x = 0$ ) with a function of the type:

$$k_{1,\text{cal}} = \frac{[\text{H}^+]_0}{1 + K [\text{H}^+]_0} \frac{\sum_{x=0}^3 k_{1,x} [\text{Cr}(\text{OH})_x (\text{H}_2\text{O})_{6-x}^{(3-x)+}]}{\sum_{x=0}^3 [\text{Cr}(\text{OH})_x (\text{H}_2\text{O})_{6-x}^{(3-x)+}]} \quad (25)$$

yielding the results  $k_{1,1} = 1.77 \text{ M}^{-1} \text{ s}^{-1}$ ,  $k_{1,2} = 128 \text{ M}^{-1} \text{ s}^{-1}$ ,  $k_{1,3} = 3.07 \times 10^4 \text{ M}^{-1} \text{ s}^{-1}$ , and  $K = 9.66 \times 10^4 \text{ M}^{-1}$ , with an excellent concordance between  $k_{1,\text{cal}}$  and  $k_{1,\text{exp}}$  (Figure 12, bottom). We can see that, according to these data, the reactivity of the chromium species toward L-alanine increases following the sequence  $\text{CrOH}^{2+} < \text{Cr}(\text{OH})_2^+ < \text{Cr}(\text{OH})_3$ , each time an aqua ligand

is replaced by a hydroxo ligand resulting in a rate constant enhancement by two orders of magnitude. This is consistent with the reported 75-fold enhancement of the reactivity toward water exchange of the hydroxopentaaqua Cr(III) complex with respect to the hexaaqua complex.<sup>55</sup>

**3.9. Mechanism.** The detected long-lived intermediate divides the reaction mechanism in two sequences, each with its own slow rate-determining step, the activation energy associated with the first sequence being the lower of the two (Figure 13). Thus, according to the available experimental data, the mechanism that can be proposed for the complexation of Cr(III) by L-alanine consists of two elementary step sequences. The first leads from the reactants to the long-lived intermediate:



where  $x = 1, 2, \text{ or } 3$ , depending on the particular reacting Cr(III) species, and RH stands for the zwitterionic form of the amino acid. The experimental results suggest that the presence of  $\text{OH}^-$  ligands in the reactant complex renders the Cr(III)- $\text{H}_2\text{O}$  chemical bonds more labile. The breakage of one of those bonds (as in eq 26) has been postulated to be a requirement for the

formation of the Cr(III)-EDTA complex.<sup>7</sup> Then, a competition between hydroxide ion (eq 27), water (eq 28) and the organic ligand (eq 29) for the vacant coordination site of the penta-coordinated metal ion takes place. In the last reaction the organic ligand suffers a conversion from monodentate (RH) to bidentate (R) and a water molecule is released, leading to the formation of the long-lived intermediate (eq 30).

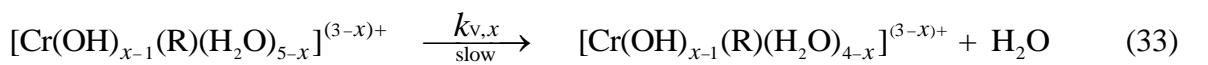
Assuming that the penta-coordinated intermediate is reactive enough to be in steady state, the following expressions can be obtained for the parameters appearing in eq 25:

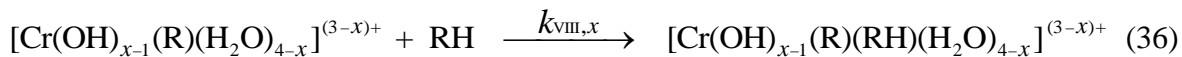
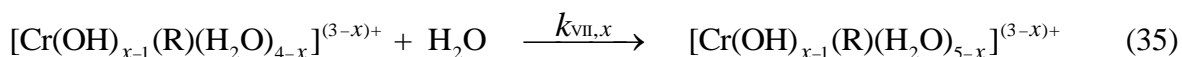
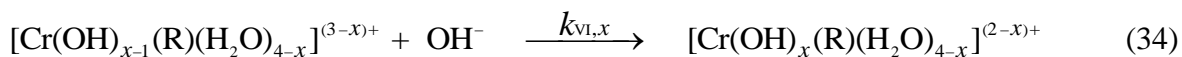
$$K = \frac{k_{\text{III},x} + k_{\text{IV},x} [\text{RH}]}{K_{\text{w}} k_{\text{II},x}} \quad (31)$$

$$k_{1,x} = \frac{k_{1,x} k_{\text{IV},x}}{K_{\text{w}} k_{\text{II},x}} [\text{RH}] \quad (32)$$

where  $K_{\text{w}}$  is the water ionic product. Equations 25, 31 and 32 are consistent with the dependence of  $k_1$  on the initial concentration of organic ligand (fractional kinetic order, Figure 4, top). Moreover, the increasing effect of the ionic strength (Figure S4, top) can be explained by the decrease of rate constant  $k_{\text{II},x}$ , since eq 27 involves two unlike-charged ions as reactants (for  $x = 1$  or 2), and the observed base catalysis (Figure 5, top) comes straightforward from the increase of  $k_{1,x}$  as  $x$  increases from 1 to 3.

The second sequence (that parallels the first one) leads from the long-lived intermediate to the reaction products:





Assuming again that the penta-coordinated intermediate is reactive enough to be in steady state, the following expression can be obtained for the second experimental rate constant:

$$k_2 = \frac{\sum_{x=1}^3 k_{2,x} [\text{Cr}(\text{OH})_{x-1}(\text{R})(\text{H}_2\text{O})_{5-x}]^{(3-x)+}}{\sum_{x=1}^3 [\text{Cr}(\text{OH})_{x-1}(\text{R})(\text{H}_2\text{O})_{5-x}]^{(3-x)+}} \quad (37)$$

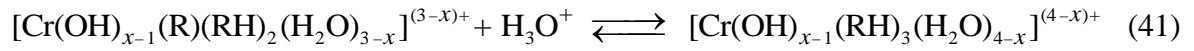
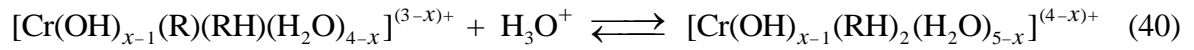
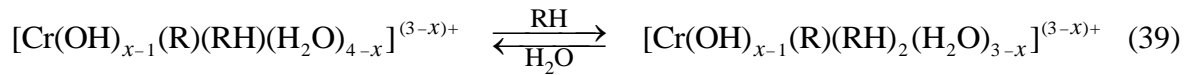
where:

$$k_{2,x} = \frac{k_{\text{V},x} k_{\text{VIII},x} [\text{RH}]}{k_{\text{VI},x} [\text{OH}^-] + k_{\text{VII},x} + k_{\text{VIII},x} [\text{RH}]} \quad (38)$$

Equations 37 and 38 are consistent with the dependence of  $k_2$  on the initial concentration of organic ligand (fractional kinetic order, Figure 4, bottom). Moreover, the decreasing effect of the ionic strength (Figure S4, bottom) and the increasing effect of the pH (Figure 5, bottom) might be explained by the change in the relative proportions of the long-lived intermediates of the type  $[\text{Cr}(\text{OH})_{x-1}(\text{R})(\text{H}_2\text{O})_{5-x}]^{(3-x)+}$ , provided that  $k_{\text{V},x}$  increases gradually from  $x = 1$  to 3 (the hydroxo ligands render the Cr-H<sub>2</sub>O bonds more labile), addition of a background

electrolyte resulting in an increase of the contributions of the less reactive, lower- $x$  species (through a shift of the acid-dissociation equilibria of the long-lived intermediates to the left side because the reaction products are like-charged ions), whereas an increase of the pH resulted in an increase of the contributions of the more reactive, higher- $x$  species.

Given enough time ( at  $t = \infty$  ), the following equilibria might be reached:



The correspondence between the complexes appearing in eqs 39 – 41 and those seen before in eqs 12 and 13 is shown in Table 4.

The number of hydrogen ions released to the medium during the course of the reaction (per chromium atom belonging to the violet complex) can then be estimated as:

$$\text{Number}(\text{H}^+) = \frac{x ([\text{C}_n] + [\text{C}_{n+1}]) + (x-1) ([\text{C}_n - \text{H}^+] + [\text{C}_{n+1} - \text{H}^+])}{[\text{Cr}(\text{III})]_{\text{T}}} \quad (42)$$

and, depending on the experimental conditions, it takes values in the range  $0 < \text{Number}(\text{H}^+) < 3$  (since  $x = 1-3$ ), in agreement with Figure 11.

Finally, we can conclude that, all in all, and considering the complexity of the chemical problem under study, the kinetic model used to obtain the reaction parameters should be considered as a good enough approximation to the real behavior of nature.

#### 4. CONCLUSIONS

(i) The reaction rate decreased much faster than expected for a pseudo-first order process (even under a large excess of organic ligand). This unusual pattern could be explained by the participation of a long-lived intermediate, not being reactive enough for the steady-state approximation to apply, and the rate constants corresponding to the formation ( $k_1$ ) and decay ( $k_2$ ) of the long-lived intermediate have been determined under different experimental conditions. (ii) Rate constant  $k_1$  was one order of magnitude higher than  $k_2$ , and the respective activation energies were  $60.2 \pm 3.3$  and  $83.3 \pm 5.9$  kJ mol<sup>-1</sup>, indicating that the formation of the long-lived intermediate was much faster than its decay. (iii) The UV-Vis spectrum of the long-lived intermediate was intermediary between those of the green inorganic reactant and the violet reaction product, whereas the spectroscopy data strongly suggested the coexistence of at least four complexes between Cr(III) and L-alanine in the final reacting mixture. (iv) The rate constants for the replacement of an aqua ligand by L-alanine followed the sequence  $\text{CrOH}^{2+} < \text{Cr(OH)}_2^+ < \text{Cr(OH)}_3$ , revealing that the hydroxo ligands rendered the Cr(III)-H<sub>2</sub>O chemical bonds more labile. (v) A reaction mechanism, consistent with the available experimental information, has been proposed, including an elementary reaction sequence for each experimental rate constant, the key (slow) steps involving the breakage of a Cr(III)-H<sub>2</sub>O chemical bond, thus leaving a vacant coordination place to allow the entrance of the organic ligand.



## ■ ASSOCIATED CONTENT

### **S** Supporting Information

The Supporting Information is available free of charge on the ACS Publications website.

- . Absorbance-absorbance plots, absorbance-time and attempted pseudo-first order plots, rate constants at various initial concentrations of metal ion and ionic strengths, Arrhenius plots for the reactions of Cr(III) with five amino acids, comparison of the reactions with L-alanine and DL-alanine, UV-Vis spectrum parameters for the final violet complex at various metal ion and potassium hydroxide initial concentrations, and relative fractions of the Cr(III)-aqua complexes as a function of the pH (PDF).

## ■ AUTHOR INFORMATION

### Corresponding Author

\* J. F. Perez-Benito: E-mail: [jfperezdebenito@ub.edu](mailto:jfperezdebenito@ub.edu).

### ORCID <sup>ID</sup>

J. F. Perez-Benito: 0000-0001-8407-3458

### Notes

The authors declare no competing financial interest.

## ■ REFERENCES

(1) Nkabinde, S. V.; Kinunda, G.; Jaganyi, D. Mechanistic Study of the Substitution Reactions of  $[\text{Pt}(\text{II})(\text{bis}(2\text{-pyridylmethyl})\text{amine})\text{H}_2\text{O}](\text{ClO}_4)_2$  and  $[\text{Pt}(\text{II})(\text{bis}(2\text{-pyridylmethyl})\text{sulfide})\text{H}_2\text{O}](\text{ClO}_4)_2$  with Azole Nucleophiles. Crystal Structure of  $[\text{Pt}(\text{II})(\text{bis}(2\text{-pyridylmethyl})\text{sulfide})\text{Cl}]\text{ClO}_4$ . *Inorg. Chim. Acta* **2017**, *466*, 298–307.

- (2) Bakac, A.; Espenson, J. H. Chromium Complexes Derived from Molecular Oxygen. *Acc. Chem. Res.* **1993**, *26*, 519–523.
- (3) Perez-Benito, J. F. Effects of Chromium(VI) and Vanadium(V) on the Lifespan of Fish. *J. Trace Elem. Med. Biol.* **2006**, *20*, 161–170.
- (4) Hamm, R. E. Complex Ions of Chromium. IV. The Ethylenediaminetetraacetic Acid Complex with Chromium(III). *J. Am. Chem. Soc.* **1953**, *75*, 5670–5672.
- (5) Perez-Benito, J. F. Two Rate Constant Kinetic Model for the Chromium(III)-EDTA Complexation Reaction by Numerical Simulations. *Int. J. Chem. Kinet.* **2017**, *49*, 234–249.
- (6) Hedrick, C. E. Formation of the Chromium-EDTA Complex. *J. Chem. Educ.* **1965**, *42*, 479–480.
- (7) Barreto, J. C.; Brown, D.; Dubetz, T.; Kakareka, J.; Alberte, R. S. A Spectrophotometric Determination of the Energy of Activation ( $E_a$ ) for a Complexation Reaction: The Kinetics of Formation of a Cr(III)/EDTA Complex. *Chem. Educator* **2005**, *10*, 196–199.
- (8) Staniek, H.; Wojaciak, R. W. The Combined Effect of Supplementary Cr(III) Propionate Complex and Iron Deficiency on the Chromium and Iron Status in Female Rats. *J. Trace Elem. Med. Biol.* **2018**, *45*, 142–149.
- (9) Schwarz, K.; Mertz, W. Chromium(III) and the Glucose Tolerance Factor. *Arch. Biochem. Biophys.* **1959**, *85*, 292–295.
- (10) Berdicevsky, I.; Mirsky, N. Effects of Insuline and Glucose-Tolerance Factor (GTF) on Growth of *Saccharomyces cerevisiae*. *Mycoses* **1994**, *37*, 405–410.
- (11) Weksler-Zangen, S.; Mizrahi, T.; Raz, I. Glucose Tolerance Factor Extracted from Yeast: Oral Insulin-Mimetic and Insulin-Potentiating: *In Vivo* and *In Vitro* Studies. *Br. J. Nutr.* **2012**, *108*, 875–882.

- (12) Liu, L.; Cui, W. M.; Zhang, S. W.; Kong, F. H.; Pedersen, M. A.; Wen, Y.; Lv, J. P. Effect of Glucose Tolerance Factor (GTF) from High Chromium Yeast on Glucose Metabolism in Insulin-Resistant 3T3-L1 Adipocytes. *RSC Adv.* **2015**, *5*, 3482–3490.
- (13) Vincent, J. B. New Evidence against Chromium as an Essential Trace Element. *J. Nutr.* **2017**, *147*, 2212–2219.
- (14) Stearns, D. M. Is Chromium a Trace Essential Metal? *Biofactors* **2000**, *11*, 149–162.
- (15) Mertz, W. Chromium in Human Nutrition. A Review. *J. Nutr.* **1993**, *123*, 626–633.
- (16) Garrett, R. H.; Grisham, C. M. *Biochemistry*; Cengage Learning: Boston, 2017.
- (17) Kitadai, N.; Oonishi, H.; Umemoto, K.; Usui, T.; Fukushi, K.; Nakashima, S. Glycine Polymerization on Oxide Minerals. *Orig. Life Evol. Biosph.* **2017**, *47*, 123–143.
- (18) Remko, M.; Rode, B. M. Catalyzed Peptide Bond Formation in the Gas Phase. Role of Bivalent Cations and Water in Formation of 2-Aminoacetamide from Ammonia and Glycine and in Dimerization of Glycine. *Struct. Chem.* **2004**, *15*, 223–232.
- (19) Khan, I. A.; Kabir-ud-Din, K. Anation of Hexaaquachromium(III) by Glycine. *J. Inorg. Nucl. Chem.* **1981**, *43*, 1082–1085.
- (20) Khan, I. A.; Shadid, M.; Kabir-ud-Din, K. Kinetics of Anation of Hexaaquachromium(III) Ion by Serine in Aqueous Acidic Medium. *Indian J. Chem. A* **1983**, *22*, 382–385.
- (21) Khan, I. A.; Kabir-ud-Din, K. Kinetics of Anation of Hexaaquachromium(III) Ion by Valine in Aqueous Acidic Medium. *Indian J. Chem. A* **1984**, *23*, 98–101.
- (22) Khan, I. A.; Kabir-ud-Din, K. Kinetics of Anation of Hexaaquachromium(III) Ion by Aspartic Acid – Mechanism and Activation Parameters. *Transition Met. Chem.* **1986**, *11*, 391–395.

- (23) Khan, I. A.; Shahid, M.; Kabir-ud-Din, K. Kinetic and Mechanistic Studies on the Complexation of Aquachromium(III) with DL-Tryptophan in Aqueous Acidic Media. *J. Chem. Soc. Dalton* **1990**, *10*, 3007–3012.
- (24) Khan, I. A.; Shahid, M.; Kabir-ud-Din, K. Methionine Anation of Aquachromium(III). *Transition Met. Chem.* **1991**, *16*, 18–22.
- (25) Guindy, N. M.; Abou-Gamra, Z. M.; Abdel-Messih, M. F. Kinetic Studies on the Complexation of Aqua Chromium(III) with DL-Leucine in Aqueous Acidic Media. *J. Chim. Phys.* **1999**, *96*, 851–864.
- (26) Guindy, N. M.; Abou-Gamra, Z. M.; Abdel-Messih, M. F. Kinetic Studies on the Complexation of Chromium(III) with some Amino Acids in Aqueous Acidic Medium. *Monatsh. Chem.* **2000**, *131*, 857–866.
- (27) Niogy, B. K.; De, G. S. Kinetics and Mechanism of Anation of Hydroxopentaaquachromium(III) Ion by DL-Phenylalanine in Aqueous Solution. *J. Indian Chem.* **1984**, *61*, 389–392.
- (28) Ramasami, T.; Taylor, R. S.; Sykes A. G. Evidence for a Dissociative Mechanism in the Reaction of Glycine with  $[\text{Cr}(\text{NH}_3)_5(\text{H}_2\text{O})]^{3+}$ . Ionic Strength Contributions (as a 1:1 Electrolyte) and Ion-Pairing ( $K_{\text{IP}}$ ) Ability of the Glycine Zwitterion. *Inorg. Chem.* **1976**, *15*, 2318–2320.
- (29) Khan, I. A.; Kabir-ud-Din, K. Studies on the Composition and Kinetics of Chromium(III)-Alanine System. *Int. J. Chem. Kinet.* **1985**, *17*, 1263–1272.
- (30) Niogy, B. K.; De, G. S. Kinetics and Mechanism of Anation of Hydroxopentaaquachromium(III) Ion by DL-Alanine in Aqueous Solution. *Proc. Indian Acad. Sci. Chem. Sci.* **1983**, *92*, 153–161.

- (31) Volk, L.; Richardson, W.; Lau, K. H.; Hall, M.; Lin, S. H. Steady State and Equilibrium Approximations in Reaction Kinetics. *J. Chem. Educ.* **1977**, *54*, 95–97.
- (32) Wilkinson, F. *Chemical Kinetics and Reaction Mechanisms*; Van Nostrand Reinhold: New York, 1980.
- (33) Perez-Benito, J. F. Some Considerations on the Fundamentals of Chemical Kinetics: Steady State, Quasi-Equilibrium, and Transition State Theory. *J. Chem. Educ.* **2017**, *94*, 1238–1246.
- (34) Freeman, F.; Kappos, J. C. Permanganate Ion Oxidations. 15. Additional Evidence for Formation of Soluble (Colloidal) Manganese Dioxide during the Permanganate Ion Oxidation of Carbon-Carbon Double Bonds in Phosphate-Buffered Solutions. *J. Am. Chem. Soc.* **1985**, *107*, 6628–6633.
- (35) Perez-Benito, J. F.; Arias, C. Occurrence of Colloidal Manganese Dioxide in Permanganate Reactions. *J. Colloid Interface Sci.* **1991**, *152*, 70–84.
- (36) Perez-Benito, J. F. Autocatalytic Reaction Pathway on Manganese Dioxide Colloidal Particles in the Permanganate Oxidation of Glycine. *J. Phys. Chem. C* **2009**, *113*, 15982–15991.
- (37) Perez-Benito, J. F.; Nicolas-Rivases, J. Kinetics of the Chromium(III)/L-Glutamic Acid Complexation Reaction: Formation, Decay, and UV-Vis Spectrum of a Long-Lived Intermediate. *Int. J. Chem. Kinet.* **2018**, *50*, 591–603.
- (38) Espenson, J. H. *Chemical Kinetics and Reaction Mechanisms*; McGraw-Hill: New York, 1995.
- (39) Stünzi, H.; Marty, W. Early Stages of the Hydrolysis of Chromium(III) in Aqueous Solution. 1. Characterization of a Tetrameric Species. *Inorg. Chem.* **1983**, *22*, 2145–2150.

- (40) Galstyan, G.; Knapp, E. W. Computing  $pK_a$  Values of Hexa-Aqua Transition Metal Complexes. *J. Comput. Chem.* **2015**, *36*, 69–78.
- (41) Carey, L. R.; Jones, W. E.; Swaddle, T. W. The Mechanisms of Substitution Reactions of Acidopentaaquochromium(III) Complexes. *Inorg. Chem.* **1971**, *10*, 1566–1570.
- (42) Guastalla, G.; Swaddle, T. W. *Cis*-Activation by Oxyanions Coordinated to Chromium(III): Aquation and Base Hydrolysis of Nitratopentaamminechromium(III) Ion. *Can. J. Chem.* **1974**, *52*, 527–535.
- (43) Krug, R. R.; Hunter, W. G.; Grieger, R. A. Statistical Interpretation of the Enthalpy-Entropy Compensation. *Nature* **1976**, *261*, 566–567.
- (44) Krug, R. R.; Hunter, W. G.; Grieger, R. A. Enthalpy-Entropy Compensation. 1. Some Fundamental Statistical Problems Associated with the Analysis of van't Hoff and Arrhenius Data. *J. Phys. Chem.* **1976**, *80*, 2335–2341.
- (45) Krug, R. R.; Hunter, W. G.; Grieger, R. A. Enthalpy-Entropy Compensation. 2. Separation of the Chemical from the Statistical Effect. *J. Phys. Chem.* **1976**, *80*, 2341–2351.
- (46) Lente, G.; Fabian, I.; Poe, A. J. A Common Misconception about the Eyring Equation. *New J. Chem.* **2005**, *29*, 759–760.
- (47) Perez-Benito, J. F. Some Tentative Explanations for the Enthalpy-Entropy Compensation Effect in Chemical Kinetics: From Experimental Errors to the Hinshelwood-Like Model. *Monatsh. Chem.* **2013**, *144*, 49–58.
- (48) Koudriavtsev, A. B.; Linert, W. Do Experimental Errors Really Cause Isoequilibrium and Isokinetic Relationships? *MATCH* **2013**, *70*, 7–28.
- (49) Linert, W.; Yelon, A. Isokinetic Relationships. *Monatsh. Chem.* **2013**, *144*, 1–2.

- (50) Perez-Benito, J. F.; Mulero-Raichs, M. Enthalpy-Entropy Compensation Effect in Chemical Kinetics and Experimental Errors: A Numerical Simulation Approach. *J. Phys. Chem. A* **2016**, *120*, 7598–7609.
- (51) Coetzee, J. F.; Ritchie, C. D. *Solute-Solvent Interactions*; Dekker: New York, 1969.
- (52) Dawson, R. M. C.; Elliott, D. C.; Elliott, W. H.; Jones, K. M. *Data for Biochemical Research*; Clarendon Press: Oxford, 1989.
- (53) Rai, D.; Sass, B. M.; Moore, D. A. Chromium(III) Hydrolysis Constants and Solubility of Chromium(III) Hydroxide. *Inorg. Chem.* **1987**, *26*, 345–349.
- (54) Lopez-Gonzalez, H.; Peralta-Videa, J. R.; Romero-Guzman, E. T.; Rojas-Hernandez, A.; Gardea-Torresdey, J. L. Determination of the Hydrolysis Constants and Solubility Product of Chromium(III) from Reduction of Dichromate Solutions by ICP-OES and UV-Visible Spectroscopy. *J. Solution Chem.* **2010**, *39*, 522–532.
- (55) Xu, F. C.; Krouse, H. R.; Swaddle, T. W. Conjugate Base Pathway for Water Exchange on Aqueous Chromium(III): Variable-Pressure and -Temperature Kinetic Study. *Inorg. Chem.* **1985**, *24*, 267–270.

---

**Table 1. Values of the Experimental Rate Constants at Various Temperatures<sup>a</sup>**

$T / ^\circ\text{C}$	$k_1 / 10^{-4} \text{ s}^{-1}$	$k_2 / 10^{-5} \text{ s}^{-1}$	$E / 10^{-4}^b$
20.0	$2.59 \pm 0.01$	$2.63 \pm 0.01$	$5.54 \pm 0.76$
22.5	$3.02 \pm 0.03$	$3.30 \pm 0.06$	$6.79 \pm 0.42$
25.0	$3.73 \pm 0.04$	$5.08 \pm 0.24$	$5.28 \pm 0.14$
27.5	$4.72 \pm 0.01$	$6.03 \pm 0.29$	$6.95 \pm 1.34$
30.0	$5.77 \pm 0.49$	$8.03 \pm 0.97$	$6.30 \pm 2.71$

<sup>a</sup>  $[\text{Cr}(\text{NO}_3)_3]_0 = 5.88 \times 10^{-3} \text{ M}$ ,  $[\text{L-alanine}]_0 = 0.354 \text{ M}$ ,  $[\text{KOH}]_0 = 5.03 \times 10^{-3} \text{ M}$ ,  $\text{pH}_\infty = 4.06 \pm$

0.03. <sup>b</sup> Average error of the calculated absorbances with respect to the experimental values.

---



**Table 2. Arrhenius and Eyring Parameters Associated with the Experimental Rate Constants with Several Biological Amino Acids as Complexing Agents<sup>a</sup>**

amino acid	rate constant	$\ln (A/s^{-1})$	$E_a / \text{kJ mol}^{-1}$	$\Delta H_{\ddagger}^{\circ} / \text{kJ mol}^{-1}$	$\Delta S_{\ddagger}^{\circ} / \text{J K}^{-1} \text{mol}^{-1}$
glycine <sup>b</sup>	$k_1$	$15.3 \pm 1.7$	$58.8 \pm 4.1$	$56.3 \pm 4.1$	$-126.1 \pm 13.8$
	$k_2$	$22.0 \pm 1.7$	$79.9 \pm 4.2$	$77.4 \pm 4.2$	$-70.7 \pm 14.2$
L-alanine <sup>c</sup>	$k_1$	$16.4 \pm 1.3$	$60.2 \pm 3.3$	$57.7 \pm 3.3$	$-116.8 \pm 11.0$
	$k_2$	$23.6 \pm 2.4$	$83.3 \pm 5.9$	$80.9 \pm 5.9$	$-56.6 \pm 19.7$
L-phenylalanine <sup>d</sup>	$k_1$	$24.3 \pm 1.7$	$83.6 \pm 4.2$	$81.1 \pm 4.2$	$-51.2 \pm 14.0$
	$k_2$	$36.5 \pm 3.5$	$117.2 \pm 8.6$	$114.8 \pm 8.6$	$50.6 \pm 28.8$
L-threonine <sup>e</sup>	$k_1$	$10.8 \pm 1.4$	$47.7 \pm 3.5$	$45.2 \pm 3.5$	$-163.6 \pm 11.9$
	$k_2$	$23.1 \pm 1.5$	$82.9 \pm 3.7$	$80.4 \pm 3.7$	$-61.0 \pm 12.5$
L-histidine <sup>f</sup>	$k_0$	$25.1 \pm 1.0$	$81.1 \pm 2.5$	$78.6 \pm 2.5$	$-44.3 \pm 8.4$
	$k_1$	$29.1 \pm 4.0$	$86.4 \pm 9.8$	$83.9 \pm 9.8$	$-11.3 \pm 33.0$
	$k_2$	$25.3 \pm 1.5$	$84.2 \pm 3.6$	$81.8 \pm 3.6$	$-42.5 \pm 12.1$

<sup>a</sup>  $[\text{Cr}(\text{NO}_3)_3]_0 = 5.88 \times 10^{-3} \text{ M}$ ,  $20.0 - 30.0 \text{ }^\circ\text{C}$ . <sup>b</sup>  $[\text{ligand}]_0 = 0.194 \text{ M}$ ,  $[\text{KOH}]_0 = 4.99 \times 10^{-3} \text{ M}$ ,  $\text{pH}_\infty 3.86 \pm 0.07$ . <sup>c</sup>  $[\text{ligand}]_0 = 0.354 \text{ M}$ ,  $[\text{KOH}]_0 = 5.03 \times 10^{-3} \text{ M}$ ,  $\text{pH}_\infty 4.06 \pm 0.03$ . <sup>d</sup>  $[\text{ligand}]_0 = 8.82 \times 10^{-2} \text{ M}$ ,  $[\text{KOH}]_0 = 4.97 \times 10^{-3} \text{ M}$ ,  $\text{pH}_\infty 3.58 \pm 0.02$ . <sup>e</sup>  $[\text{ligand}]_0 = 0.194 \text{ M}$ ,  $[\text{KOH}]_0 = 5.01 \times 10^{-3} \text{ M}$ ,  $\text{pH}_\infty 3.60 \pm 0.05$ . <sup>f</sup>  $[\text{ligand}]_0 = 0.119 \text{ M}$ ,  $[\text{HCl}]_0 = 9.55 \times 10^{-2} \text{ M}$ ,  $\text{pH}_\infty 4.45 \pm 0.06$ .

**Table 3. Spectral Parameters Associated with the First and Second UV-Vis Peaks of the Green (Reactant) and Violet (Product) Complexes at 25.0 °C<sup>a,b,c,d</sup>**

peak parameter	reactant <sup>e</sup>	product <sup>f</sup>
$\lambda_1 / \text{nm}$	421 (412)	391 (388)
$\lambda_2 / \text{nm}$	581 (564)	530 (522)
$\varepsilon_1 / \text{M}^{-1} \text{cm}^{-1}$	22.2 (23.3)	70.4 (82.0)
$\varepsilon_2 / \text{M}^{-1} \text{cm}^{-1}$	12.2 (19.2)	83.4 (89.4)

<sup>a</sup> The main values were obtained by extrapolation at infinite initial concentrations of either metal ion (reactant) or amino acid (product). <sup>b</sup> The values in parenthesis were obtained by extrapolation at zero initial concentrations of either metal ion (product) or amino acid (reactant). <sup>c</sup> Changing the metal ion initial concentration:  $[\text{Cr}(\text{NO}_3)_3]_0 = (0.29 - 1.76) \times 10^{-2}$  M,  $[\text{L-alanine}]_0 = 0.354$  M,  $[\text{KOH}]_0 = 5.03 \times 10^{-3}$  M,  $\text{pH}_\infty = 3.72 - 4.12$ . <sup>d</sup> Changing the amino acid initial concentration:  $[\text{Cr}(\text{NO}_3)_3]_0 = 5.88 \times 10^{-3}$  M,  $[\text{L-alanine}]_0 = 0.015 - 0.354$  M,  $[\text{KOH}]_0 = 8.28 \times 10^{-3}$  M,  $\text{pH}_\infty = 3.84 - 4.25$ . <sup>e</sup> Spectral parameters for the reactant Cr(III) coordinated to zero organic ligands. <sup>f</sup> Spectral parameters for the product Cr(III) coordinated to the highest possible number of organic ligands (saturated).

---

**Table 4. Correspondence between the Final Violet Complexes Predicted from their Recorded UV-Vis Spectra and the Chemical Formulas Proposed in the Mechanism**

predicted complex <sup>a</sup>	proposed complex <sup>b</sup>
$C_n$	$[\text{Cr}(\text{OH})_{x-1}(\text{R})(\text{RH})(\text{H}_2\text{O})_{4-x}]^{(3-x)+}$
$C_n - \text{H}^+$	$[\text{Cr}(\text{OH})_{x-1}(\text{RH})_2(\text{H}_2\text{O})_{5-x}]^{(4-x)+}$
$C_{n+1}$	$[\text{Cr}(\text{OH})_{x-1}(\text{R})(\text{RH})_2(\text{H}_2\text{O})_{3-x}]^{(3-x)+}$
$C_{n+1} - \text{H}^+$	$[\text{Cr}(\text{OH})_{x-1}(\text{RH})_3(\text{H}_2\text{O})_{4-x}]^{(4-x)+}$

<sup>a</sup> The subscripts  $n$  and  $n+1$  stand for the number of organic ligands. <sup>b</sup> RH and R stand for amino acid molecules acting as mono- or bi-dentate ligands, respectively.

---

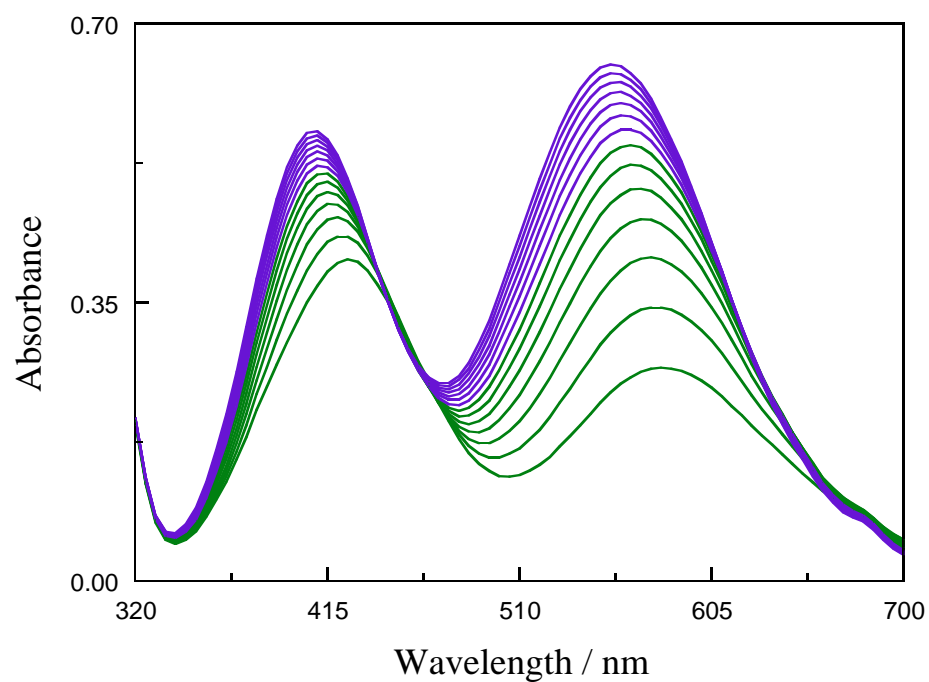


**Figure 1.** Periodic scanning of the UV-Vis spectrum at 30-min time intervals during the course of the process. The shift from green to violet indicates the progress of the reaction from reactants to products.  $[\text{Cr}(\text{NO}_3)_3]_0 = 1.76 \times 10^{-2} \text{ M}$ ,  $[\text{L-alanine}]_0 = 0.354 \text{ M}$ ,  $[\text{KOH}]_0 = 5.03 \times 10^{-3} \text{ M}$ ,  $\text{pH}_0 = 3.71$ ,  $25.0 \text{ }^\circ\text{C}$ .

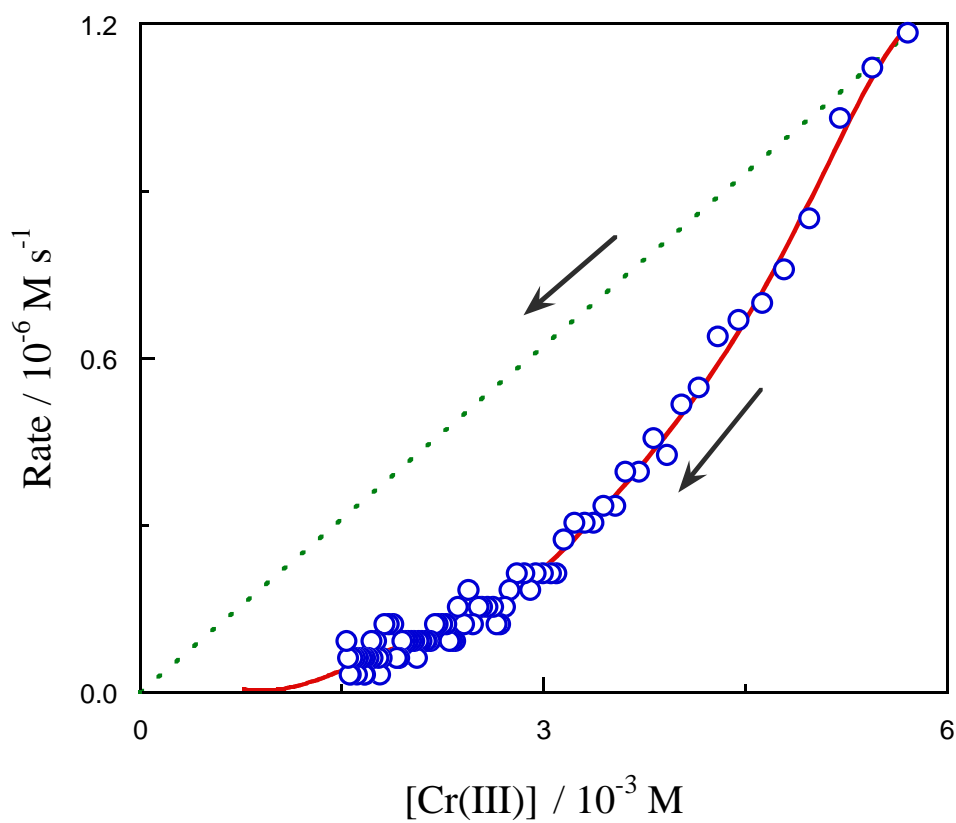


**Figure 2.** Reaction rate as a function of the limiting reactant concentration. The dashed line corresponds to a hypothetical pseudo-first order behavior, whereas the arrows indicate the progression of the complexation process.  $[\text{Cr}(\text{NO}_3)_3]_0 = 5.88 \times 10^{-3} \text{ M}$ ,  $[\text{L-alanine}]_0 = 0.133 \text{ M}$ ,  $[\text{KOH}]_0 = 8.28 \times 10^{-3} \text{ M}$ ,  $\text{pH}_\infty 3.97$ ,  $25.0 \text{ }^\circ\text{C}$ .

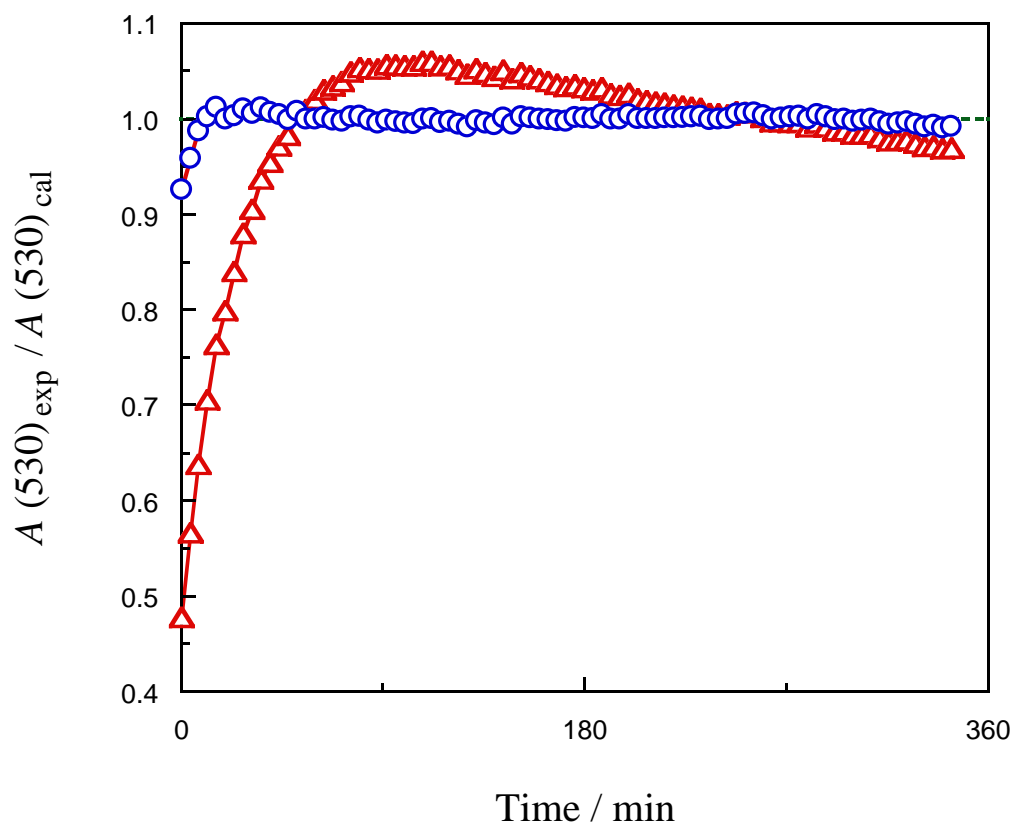


**Figure 3.** Ratio between the experimental and calculated absorbances at 530 nm as a function of time during the course of the reaction. Triangles: biparametric (pseudo-first order) kinetic model ( $E = 9.17 \times 10^{-3}$ ). Circles: tetraparametric (two rate constant) kinetic model ( $E = 7.30 \times 10^{-4}$ ).  $[\text{Cr}(\text{NO}_3)_3]_0 = 5.88 \times 10^{-3}$  M,  $[\text{L-alanine}]_0 = 0.133$  M,  $[\text{KOH}]_0 = 8.28 \times 10^{-3}$  M,  $\text{pH}_\infty$  3.97, 25.0 °C.

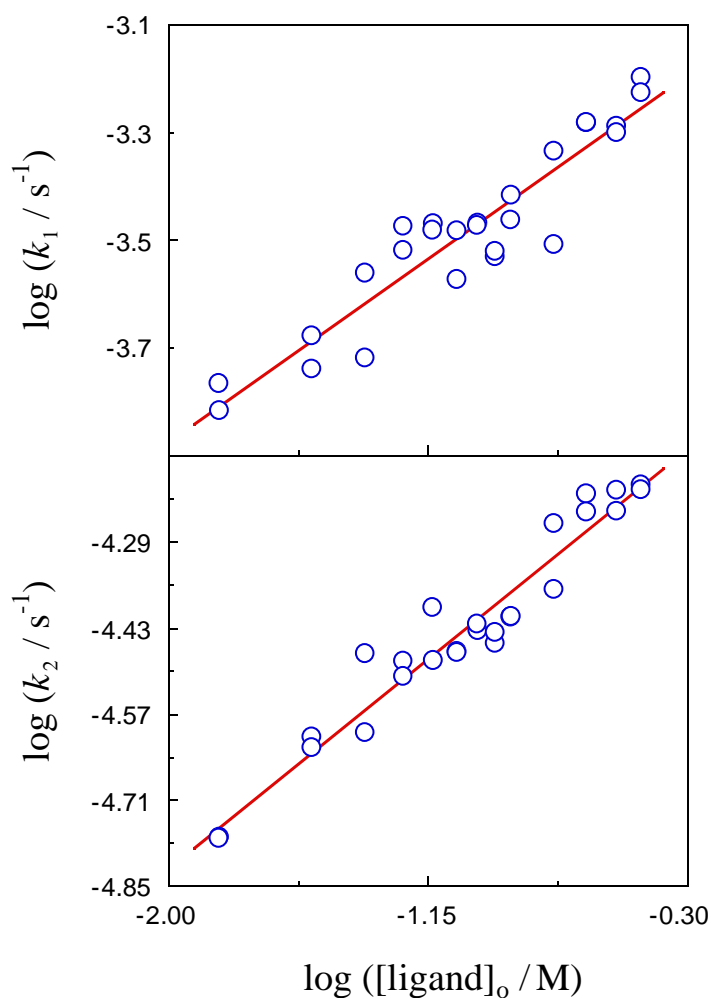


**Figure 4.** Double-logarithm plots showing the dependence of the experimental rate constants  $k_1$  (top,  $r = 0.940$ ) and  $k_2$  (bottom,  $r = 0.969$ ) on the initial concentration of L-alanine.  $[\text{Cr}(\text{NO}_3)_3]_o = 5.88 \times 10^{-3} \text{ M}$ ,  $[\text{L-alanine}]_o = 0.015 - 0.354 \text{ M}$ ,  $[\text{KOH}]_o = 8.28 \times 10^{-3} \text{ M}$ ,  $\text{pH}_\infty = 3.79 - 4.24$ ,  $25.0 \text{ }^\circ\text{C}$ .

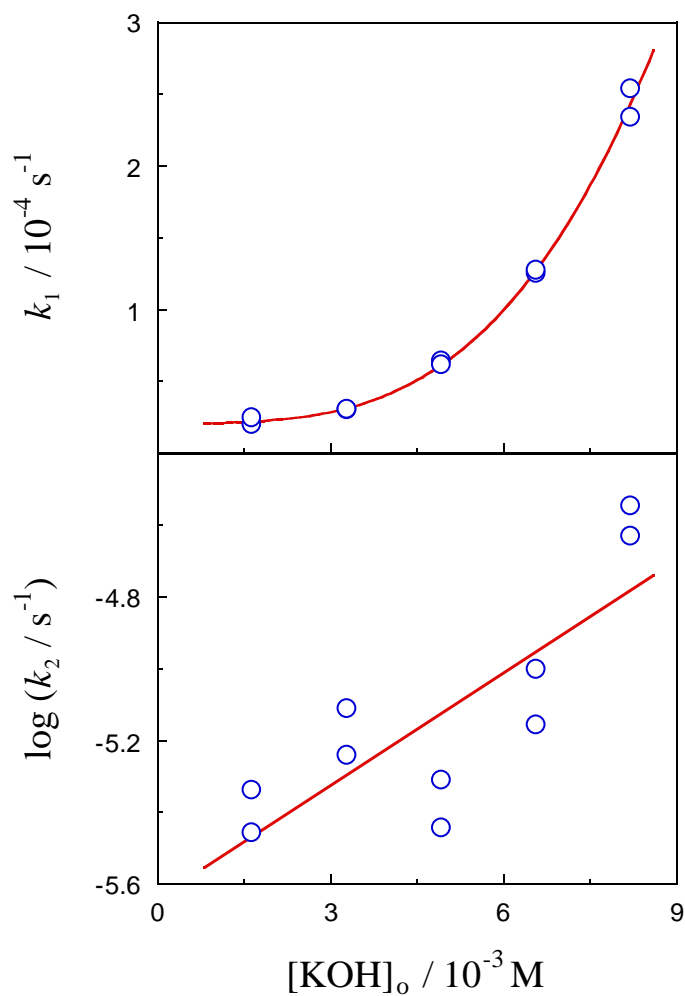


**Figure 5.** Dependence of experimental rate constants  $k_1$  (top,  $r = 0.999$ ) and  $k_2$  (bottom,  $r = 0.808$ ) on the initial concentration of potassium hydroxide.  $[\text{Cr}(\text{NO}_3)_3]_o = 5.88 \times 10^{-3} \text{ M}$ ,  $[\text{L-alanine}]_o = 5.89 \times 10^{-2} \text{ M}$ ,  $[\text{KOH}]_o = (1.64 - 8.21) \times 10^{-3} \text{ M}$ ,  $\text{pH}_o = 3.56 - 3.84$ ,  $25.0 \text{ }^\circ\text{C}$ .



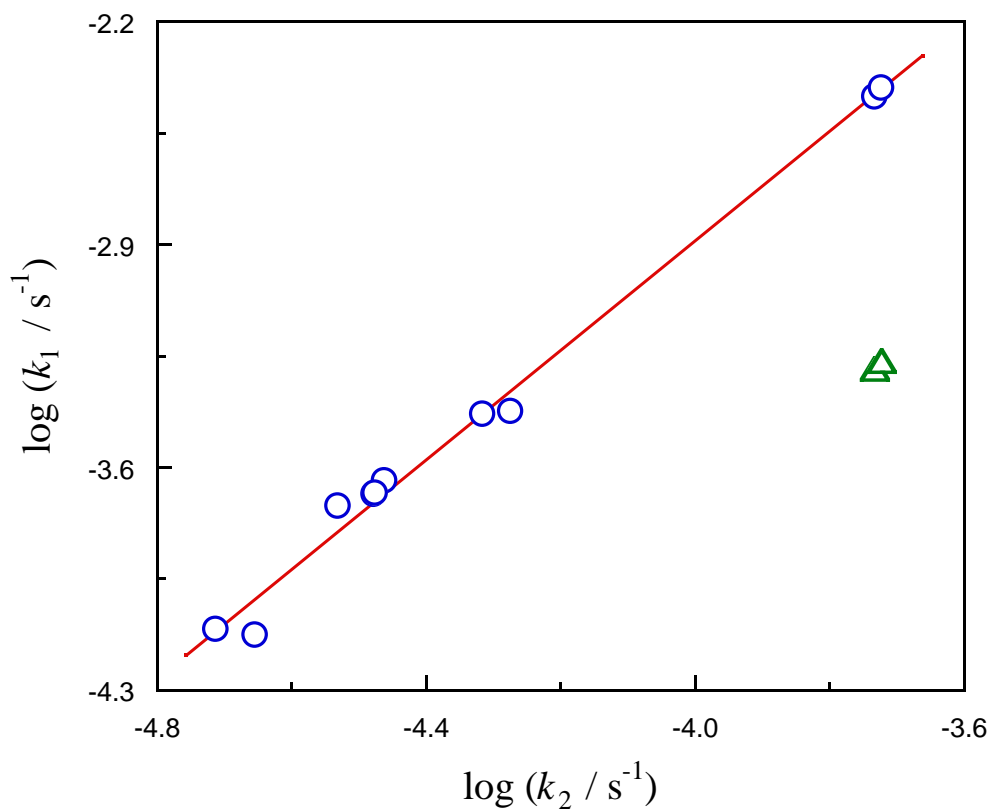


**Figure 6.** Correlation between the values of the experimental rate constants at 25.0 °C for the same amino acid. Triangles:  $k_0$  vs  $k_2$  (ligand: L- histidine). Circles:  $k_1$  vs  $k_2$  (ligands: glycine, L-alanine, L-phenylalanine, L-threonine, and L-histidine;  $r = 0.996$ ).

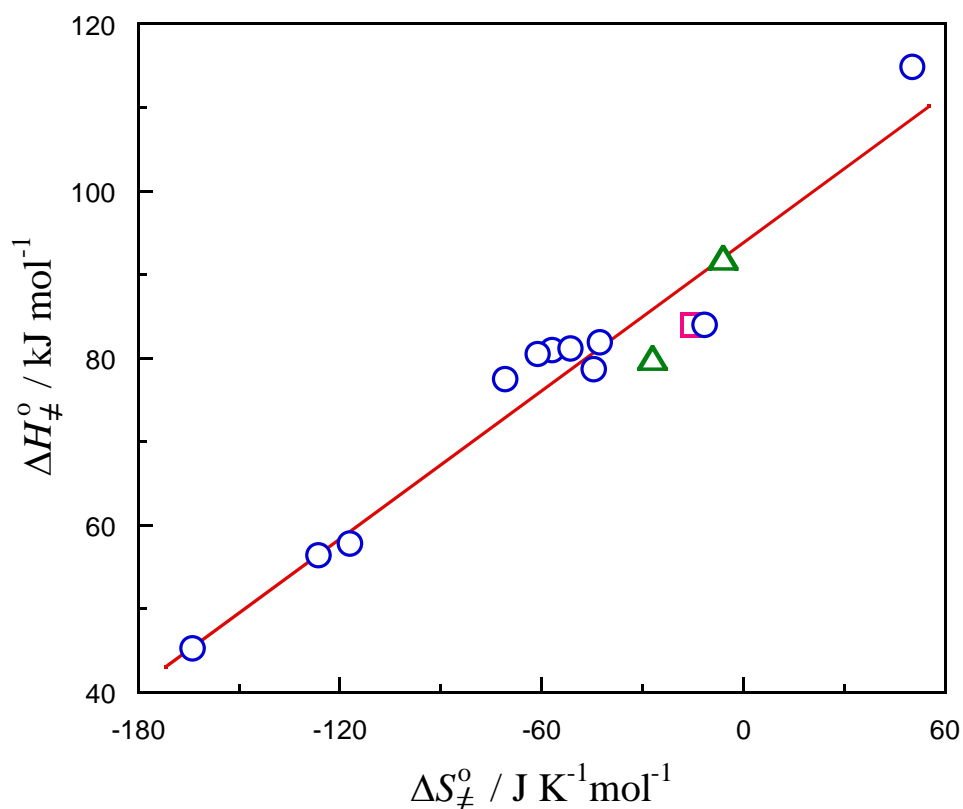


**Figure 7.** Enthalpy-entropy compensation plot for the reactions of Cr(III) with several organic ligands ( $r = 0.970$ ). Purple point: data from ref. 5 (ligand: EDTA). Green points: data from ref. 37 (ligand: L-glutamic acid). Blue points: data from this work (ligands: glycine, L-alanine, L-phenylalanine, L-threonine, and L-histidine).

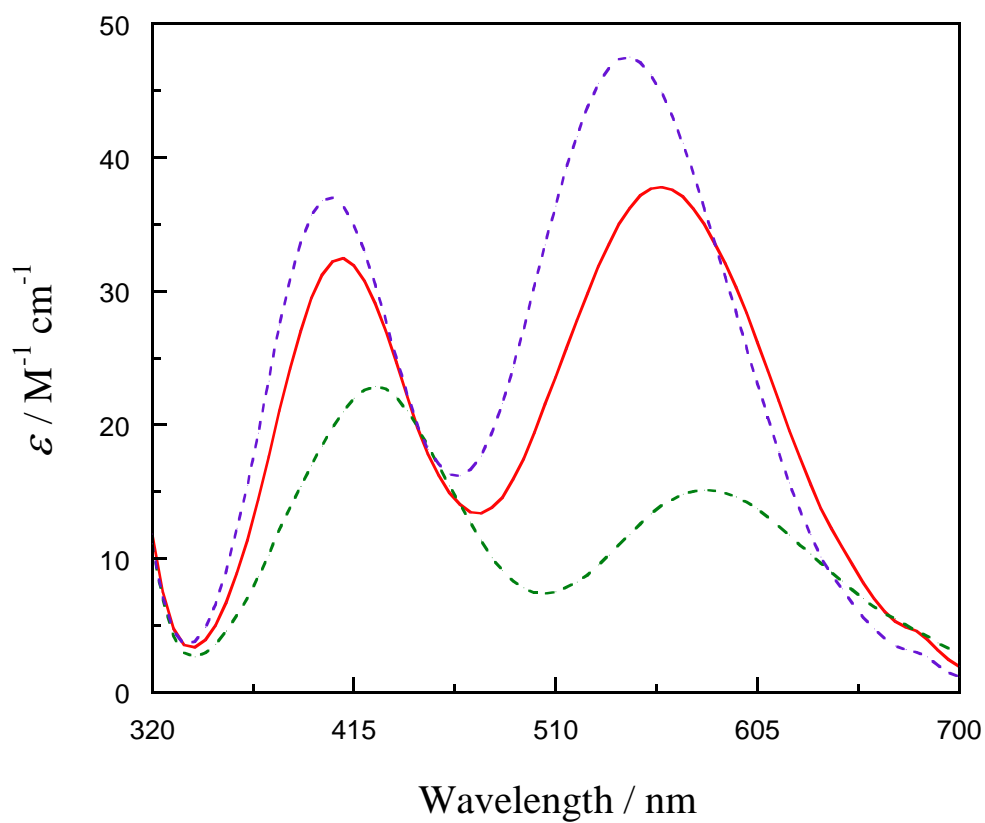


**Figure 8.** Molar absorption coefficients as a function of the wavelength for three Cr(III) complexes: reactant (green dashed line), long-lived intermediate (red continuous line), and final product (violet dashed line).  $[Cr(NO_3)_3]_0 = 1.76 \times 10^{-2}$  M,  $[L\text{-alanine}]_0 = 0.354$  M,  $[KOH]_0 = 5.03 \times 10^{-3}$  M,  $pH_\infty$  3.71, 25.0 °C.

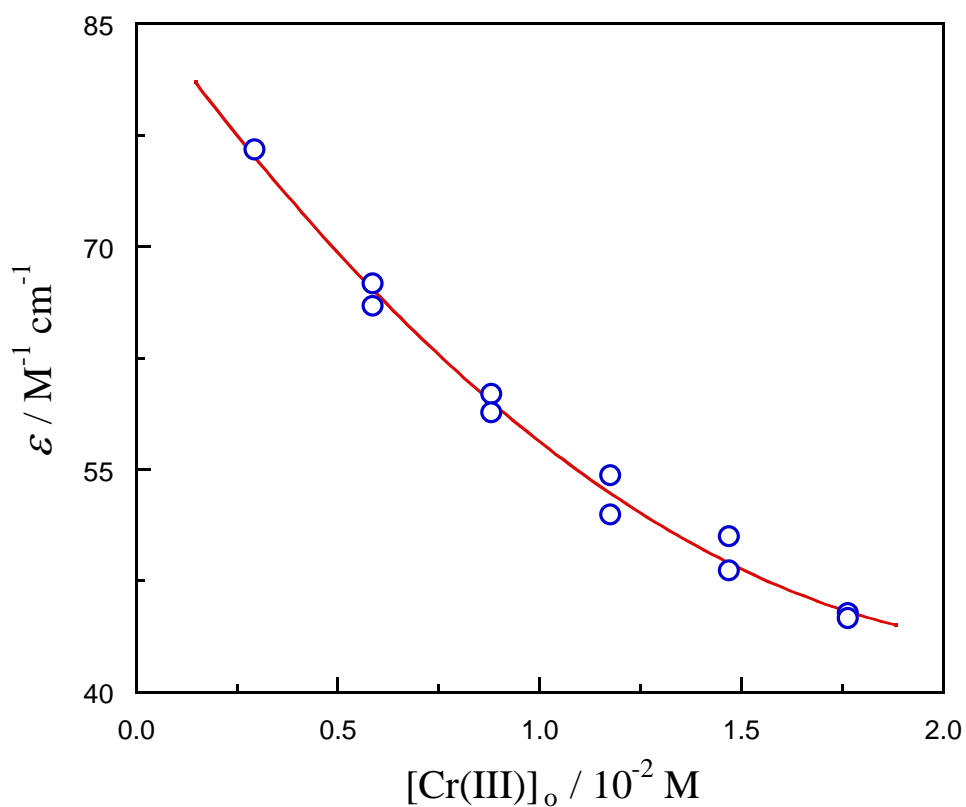


**Figure 9.** Molar absorption coefficient at 530 nm for the electronic spectrum recorded for the final violet complex as a function of the metal ion initial concentration.  $[\text{Cr}(\text{NO}_3)_3]_0 = (0.29 - 1.76) \times 10^{-2} \text{ M}$ ,  $[\text{L-alanine}]_0 = 0.354 \text{ M}$ ,  $[\text{KOH}]_0 = 5.03 \times 10^{-3} \text{ M}$ ,  $\text{pH}_\infty = 3.72 - 4.12$ ,  $25.0 \text{ }^\circ\text{C}$ .

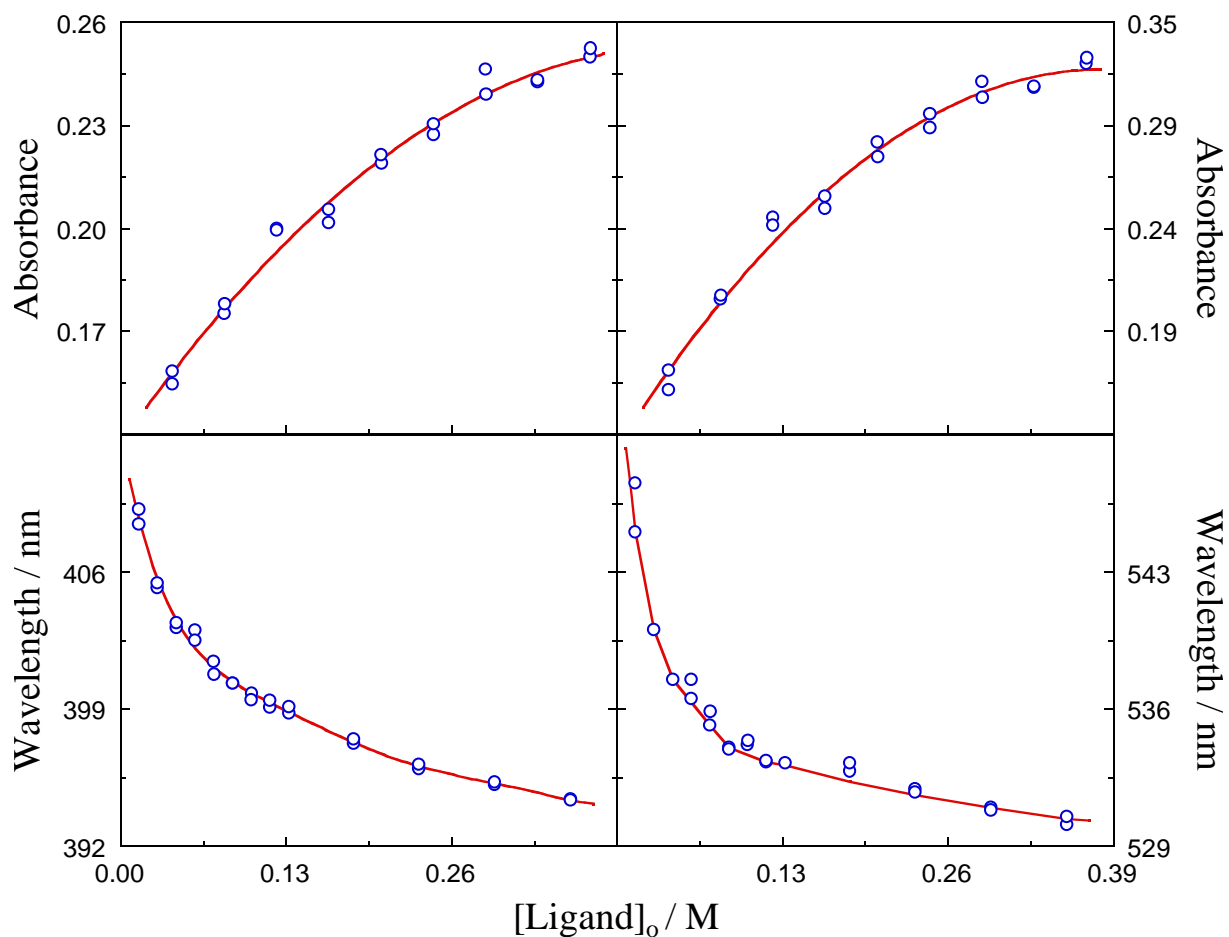


**Figure 10.** Wavelengths (bottom) and absorbances (top) corresponding to the first (left) and second (right) peaks of the electronic spectrum recorded for the final violet complex as a function of the organic ligand initial concentration.  $[\text{Cr}(\text{NO}_3)_3]_0 = 5.88 \times 10^{-3} \text{ M}$ ,  $[\text{L-alanine}]_0 = 0.015 - 0.354 \text{ M}$ ,  $[\text{KOH}]_0 = 8.28 \times 10^{-3} \text{ M}$ ,  $\text{pH}_\infty = 3.84 - 4.25$ ,  $25.0 \text{ }^\circ\text{C}$ .

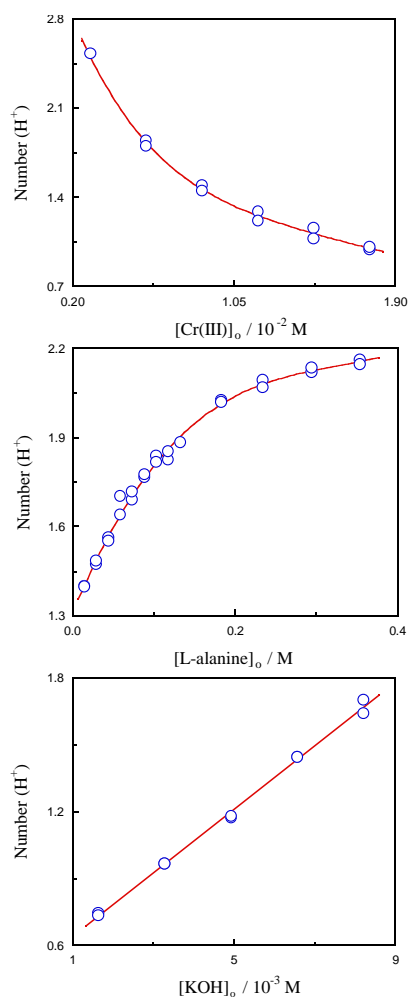


**Figure 11.** Number of hydrogen ions released per chromium atom during the course of the reaction under different experimental conditions at 25.0 °C. Top:  $[\text{Cr}(\text{NO}_3)_3]_0 = (0.29 - 1.76) \times 10^{-2}$  M,  $[\text{L-alanine}]_0 = 0.354$  M,  $[\text{KOH}]_0 = 5.03 \times 10^{-3}$  M,  $\text{pH}_\infty$  3.72–4.12. Middle:  $[\text{Cr}(\text{NO}_3)_3]_0 = 5.88 \times 10^{-3}$  M,  $[\text{L-alanine}]_0 = 0.015 - 0.354$  M,  $[\text{KOH}]_0 = 8.28 \times 10^{-3}$  M,  $\text{pH}_\infty$  3.84–4.25. Bottom:  $[\text{Cr}(\text{NO}_3)_3]_0 = 5.88 \times 10^{-3}$  M,  $[\text{L-alanine}]_0 = 5.89 \times 10^{-2}$  M,  $[\text{KOH}]_0 = (1.64 - 8.21) \times 10^{-3}$  M,  $\text{pH}_\infty$  3.55–3.84.

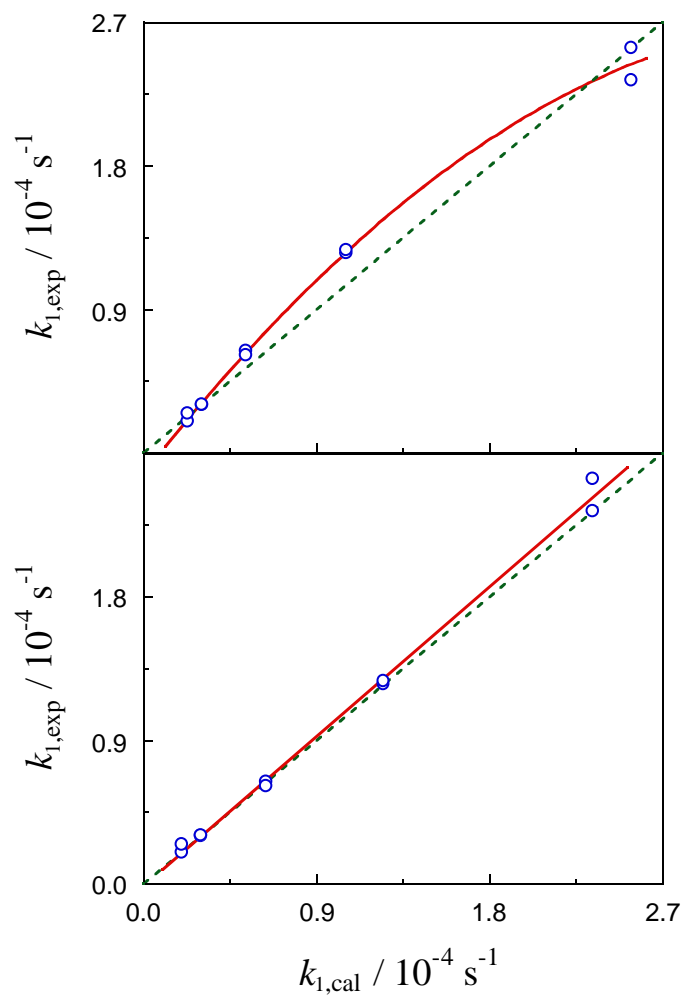


**Figure 12.** Correspondence between the experimental values of the first rate constant and those calculated according to either eq 24 (top) or eq 25 (bottom).  $[\text{Cr}(\text{NO}_3)_3]_0 = 5.88 \times 10^{-3}$  M,  $[\text{L-alanine}]_0 = 5.89 \times 10^{-2}$  M,  $[\text{KOH}]_0 = (1.64 - 8.21) \times 10^{-3}$  M,  $\text{pH}_\infty = 3.56 - 3.84$ ,  $25.0 \text{ }^\circ\text{C}$ .

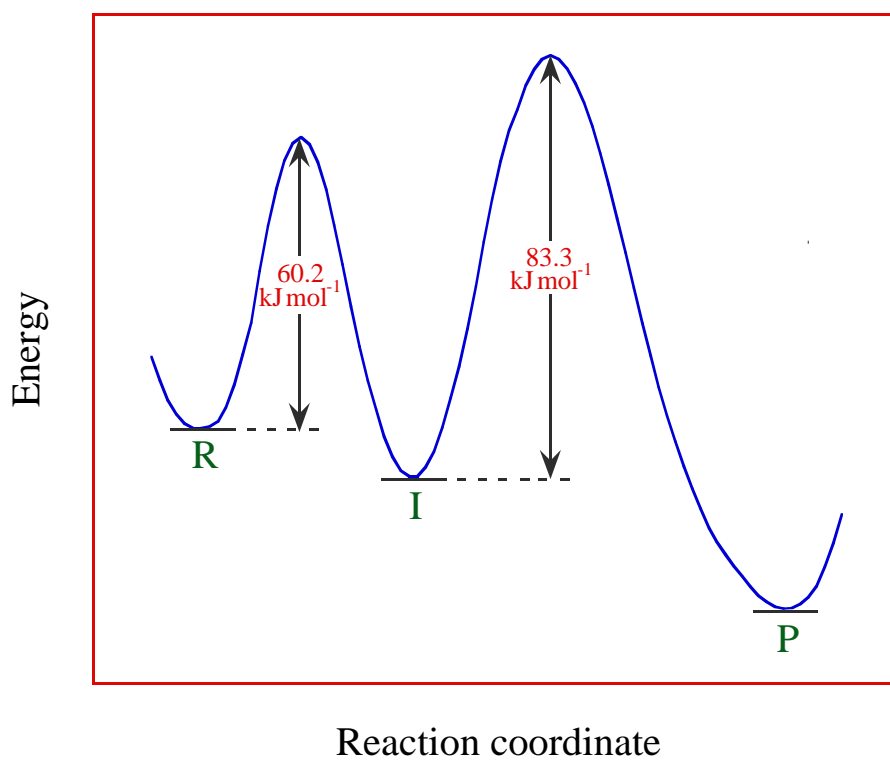


**Figure 13.** Qualitative energy-reaction coordinate diagram for the sequential complexation of Cr(III) by L-alanine showing the experimental activation energies corresponding to the conversions of the initial reactant (R) into the long-lived intermediate (I), and of the latter into the final product (P).



## Table of Contents Graphic

